†Work sponsored by the Department of the Air Force.

[1]T. B. Reed and R. E. Fahey, J. Cryst. Growth (to be published).

[2]K. Dwight, N. Menyuk, and D. Smith, J. Appl. Phys. 29, 491 (1958).

[3]M. Rayl and P. J. Wojtowicz, Phys. Letters 28A, 142 (1968).

[4]J. S. Kouvel and M. E. Fisher, Phys. Rev. 136, A1626 (1964).

[5]B. Widom, J. Chem. Phys. 43, 3898 (1965).

[6]M. E. Fisher, J. Appl. Phys. 38, 981 (1967).

[7]L. P. Kadanoff, W. Götze, D. Hamblen, R. Hecht, E. A. S. Lewis, V. V. Palciauskas, M. Rayl, J. Swift, D. Aspnes, and J. Kane, Rev. Mod. Phys. 39, 395 (1967).

[8]R. B. Griffiths, Phys. Rev. 158, 176 (1967).

[9]D. T. Teaney, in *Critical Phenomena*, edited by S. Green and V. Sengers (Natl. Bur. Std., U. S. GPO, Washington, D. C., 1965), pp. 50–57.

[10]J. T. Ho and J. D. Litster, Phys. Rev. Letters 22, 603 (1969).

[11]P. Schofield, J. D. Litster, and J. T. Ho, Phys. Rev. Letters 23, 1098 (1969).

[12]P. Schofield, Phys. Rev. Letters 22, 606 (1969).

[13]P. J. Wojtowicz and R. J. Joseph, Phys. Rev. 135, A1314 (1964).

[14]N. W. Dalton, Proc. Phys. Soc. (London) 88, 659 (1966).

[15]K. Pirnie and P. J. Wood, Phys. Letters 17, 241 (1965).

[16]K. Pirnie, P. J. Wood, and J. Eve, Mol. Phys. 11, 551 (1966).

[17]T. R. McGuire, B. E. Argyle, M. W. Shafer, and J. S. Smart, Appl. Phys. Letters 1, 17 (1962).

[18]K. Dwight and N. Menyuk (unpublished).

[19]E. L. Boyd, Phys. Rev. 145, 174 (1966).

[20]A. J. Henderson, Jr., G. R. Brown, T. B. Reed, and H. Meyer, J. Appl. Phys. 41, 946 (1970).

[21]H. E. Stanley, Phys. Rev. 158, 546 (1967).

[22]D. W. Wood and N. W. Dalton, Phys. Rev. 159, 384 (1967).

[23]R. B. Griffiths, Phys. Rev. Letters 24, 1479 (1970).

[24]The possibility of a ferromagnetic next-nearest-neighbor interaction in EuO was noted by T. Kasuya [IBM J. Res. Develop. 14, 214 (1970)]. He found such an interaction could arise from the cross term between the Kramers-Anderson (p,f) mechanism and a d,f exchange interaction.

[25]Unresolved disagreements between the values of exchange constants determined by low-temperature specific-heat measurements and Curie-point measurements have appeared previously in the literature. Specific-heat measurements in magnetite [J. S. Kouvel, Phys. Rev. 102, 1489 (1956)] and in ferrites of nickel, lithium, and cobalt [S. R. Pollack and K. R. Atkins, Phys. Rev. 125, 1248 (1962)] predicted Curie points which were approximately one-third the measured value.

[26]R. Stevenson and M. C. Robinson, Can. J. Phys. 43, 1744 (1965).

[27]G. K. Sokolova, K. M. Demshuk, K. P. Rodionov, and A. A. Samokhvalov, Zh. Eksperim. i Teor. Fiz. 49, 452 (1965) [Soviet Phys. JETP 22, 317 (1966)].

[28]D. B. McWhan, P. C. Souers, and G. Jura, Phys. Rev. 143, 385 (1966).

[29]S. H. Charap and E. L. Boyd, Phys. Rev. 133, A811 (1964).

PHYSICAL REVIEW B VOLUME 3, NUMBER 5 1 MARCH 1971

Cooperative Dynamic Jahn-Teller Effect. II. Crystal Distortion in Perovskites

B. Halperin and R. Englman
Soreq Nuclear Research Centre, Yavne, Israel
(Received 5 August 1970)

A molecular-field-type theory is given for the second-order phase transitions occurring in perovskite crystals, in which a Jahn-Teller (JT) ion (Mn^{3+}, Cu^{2+}, Cr^{2+}) occupies an octahedral B site. The dynamic character of the JT effect is taken into account and excited vibronic states are included. The ordered system consists of two sublattices, each having the same tetragonal, but opposite orthorhombic, mean distortion amplitudes. Near the transition temperature T_t, the two amplitudes behave as $T_t - T$ and $(T_t - T)^{1/2}$, respectively. Increasing the anisotropic JT coupling β enhances the mean tetragonal distortion amplitude and diminishes the orthorhombic one. The transition temperature is studied as a function of the molecular field strength and of β, and characteristic regions of solutions are distinguished. The temperature dependence of the specific heat for some typical systems is presented.

I. INTRODUCTION

In a previous paper[1] (henceforth referred to as I), a theory of cubic-to-tetragonal phase transformations in spinels due to a cooperative Jahn-Teller (JT) effect has been given. Compared to spinels, the experimental material[2–14] concerning JT-induced transformations in perovskitelike compounds is less extensive. On the other hand, in the perovskites there exists rather definite experimental evidence from the anisotropic ESR spectra due to Cu^{2+} in low concentrations,[15] that there are individual distorted JT centers even in the cubic phase.

Perovskites are seldom found to have a simple cubic structure; owing to packing-induced distor-

tions, their usual symmetry is either orthorhombic or rhombohedral, depending, e.g., upon the relative sizes of the ions.[4,6,14] Thus, the cooperative JT effect plays only a partial role in most of the observed distortions.

The problem was already discussed by Kanamori,[3] who predicted the existence of a structural phase transformation of the second order and an "antiferromagnetic" type of distortion, introducing a fictitious spin to specify the degenerate orbital states. However, in this treatment, neither the dynamic nature of the effect nor the excited vibronic states was taken into account. The influence of the anistropic energy was only qualitatively discussed by him.

The static JT effect appears to be exceptional particularly in cooperative manifestations of the effect, where a given amount of distortion is shared among a great number of modes of the lattice. This justifies, in our view, the reconsideration of the problem through a dynamic treatment.

In the higher-lying vibronic states the system tends to resonate between three equivalent distortions, one along each of the cubic axes. Raising the temperature so as to populate these states will have a disordering effect. This effect is additional to that acting within the lowest states which achieves disorder through increase of the entropy. The inclusion of excited states leads then to a reduction of the transition temperature.

In this work the problem of the cooperative JT effect is treated using the molecular-field approximation. We consider the cases in which the collective effect arises due to paramagnetic cations Mn^{3+}, Cr^{2+}, and Cu^{2+} in a doubly degenerate electronic state, situated at the octahedrally coordinated sites of the perovskite.

The static cooperative treatment is worked out in Sec. II, and effective coupling terms between adjacent octahedra are obtained. Section III is devoted to the dynamic JT treatment of the cooperative process. This amounts to solving the vibronic equation of state of each JT octahedron in the presence of interactions with its surroundings. The thermodynamics of the phase transition, the behavior of the order parameters as functions of the temperature, and the type of distortion occurring in the critical- and low-temperature regions is discussed in Sec. IV. In Sec. V, we examine the range of variation of the transition temperature and introduce five categories into which the systems may fall depending on the values of the physical parameters.

II. STATIC JAHN-TELLER TREATMENT IN PEROVSKITES: EFFECTIVE COUPLING

In Fig. 1, the $\vec{n}$th unit cell in the perovskite ABO_3 is described by the cube drawn by broken lines. For simplicity the crystal is assumed to be cubic in the absence of the JT effect and packing-induced distortions are ignored.

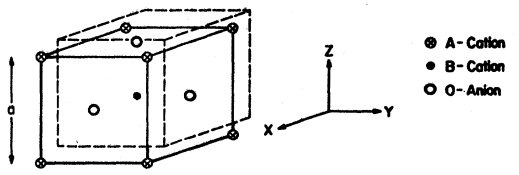

FIG. 1. Structure of a cubic ABO_3 perovskite. Cube drawn by broken lines houses one formula unit.

There are three oxygen ions in the unit cell, placed along the positive directions of the x, y, z axes, the origin of which is the B cation. The electronic state of this cation is supposed to be doubly degenerate in its cubic surroundings with components $|E_\theta\rangle$ and $|E_\epsilon\rangle$ which transform as $(2z^2-x^2-y^2)/\sqrt{6}$ and $(x^2-y^2)/\sqrt{2}$, respectively.

The Hamiltonian of the system includes the elastic energy due to the interactions of nearest and next-nearest neighbors, and the JT term. At this stage, the static limit is treated so that the kinetic-energy term is excluded.

We designate the two Pauli matrices

$$\begin{pmatrix} -1 & 0 \\ 0 & 1 \end{pmatrix}, \quad \begin{pmatrix} 0 & 1 \\ 1 & 0 \end{pmatrix}$$

by $\sigma_\theta(\vec{n})$ and $\sigma_\epsilon(\vec{n})$, respectively, which operate in the degenerate electronic function space of the B cation located in the $\vec{n}$th unit cell. The small Cartesian displacements of the ions are denoted by $X(\vec{n}, i)$, etc. Here i takes the values 1, 2, 3 when referring to the three oxygen anions which are directed along the x, y, and z axes, respectively, and the value 0 for the B cation in the $\vec{n}$th unit cell.

We thus get a sum over all unit cells of terms like

$$\tfrac{1}{2}M\omega^2\{[X(\vec{n},1)-X(\vec{n},0)]^2+[X(\vec{n}-\hat{x}a,1)-X(\vec{n},0)]^2\}$$
$$+\tfrac{1}{2}M_c\omega_c^2[X(\vec{n},0)-X(\vec{n}+\hat{x}a,0)]^2,$$

and analogous terms for the y and z directions:

$$+\tfrac{1}{2}L(M\omega/\hbar)^{1/2}\,((12)^{-1/2}\sigma_\theta(\vec{n})\{2[Z(\vec{n},3)-Z(\vec{n}-\hat{z}a,3)]$$
$$-[X(\vec{n},1)-X(\vec{n}-\hat{x}a,1)]-[Y(\vec{n},2)-Y(\vec{n}-\hat{y}a,2)]\}$$
$$+\tfrac{1}{2}\sigma_\epsilon(\vec{n})\{[X(\vec{n},1)-X(\vec{n}-\hat{x}a,1)]$$
$$-[Y(\vec{n},2)-Y(\vec{n}-\hat{y}a,2)]\}). \qquad (1)$$

$M\omega^2$ denotes the force constant for the oxygen-metal motion, while $M_c\omega_c^2$ denotes the force con-

stant for the motion of the B cations with respect to each other. The linear JT coefficient L has already been discussed in I.

The static treatment then amounts to extremization of (1) with respect to the relative displacements $X(\vec{n}, 1) - X(\vec{n}, 0)$, etc. The following coupling terms between neighboring centers are found {as multiples of $[M_c\omega_c^2/(M\omega^2 + 2M_c\omega_c^2)]L^2/12\hbar\omega$}:

coupling between $\vec{n} - \vec{n} + \hat{z}a$:

$$\sigma_\theta(\vec{n})\sigma_\theta(\vec{n} + \hat{z}a);$$

coupling between $\vec{n} - \vec{n} + \hat{x}a$:

$$[-\tfrac{1}{2}\sigma_\theta(\vec{n}) + \tfrac{1}{2}\sqrt{3}\sigma_\epsilon(\vec{n})][-\tfrac{1}{2}\sigma_\theta(\vec{n} + \hat{x}a) + \tfrac{1}{2}\sqrt{3}\sigma_\epsilon(\vec{n} + \hat{x}a)]; \tag{2}$$

coupling between $\vec{n} - \vec{n} + \hat{y}a$:

$$[-\tfrac{1}{2}\sigma_\theta(\vec{n}) - \tfrac{1}{2}\sqrt{3}\sigma_\epsilon(\vec{n})][-\tfrac{1}{2}\sigma_\theta(\vec{n} + \hat{y}a) - \tfrac{1}{2}\sqrt{3}\sigma_\epsilon(\vec{n} + \hat{y}a)].$$

The expressions within the square brackets in the last two lines are $\sigma_\theta(\vec{n})$ quantized along the direction of the line connecting the two neighboring cations, respectively, and expressed in terms of the matrices which are quantized along the z direction.

The formal analogy of the resulting coupling terms (2) with an anisotropic Heisenberg Hamiltonian has already been noted in I concerning the spinel problem. In the present case, the coupling is highly anisotropic and, so to say, antiferrodistortive. The last feature is obviously because of the fact that an oxygen which moves towards a B cation on its right necessarily moves away from the cation on its left, provided that the cation-cation force constants are not too small. When $M_c\omega_c^2$ becomes negligible, the coupling disappears.

From the antiferrodistortive nature of the coupling it is natural to assume that the lattice of the B cations may be divided into two sublattices each exhibiting, on the average, a distortion of the oxygen octahedra along a different axis. We label the two sublattices by (+) and (−) signs and denote the average values of the Pauli matrices by $\bar{\sigma}_\theta(+)$, $\bar{\sigma}_\epsilon(+)$, $\bar{\sigma}_\theta(-)$, and $\bar{\sigma}_\epsilon(-)$. We also assume the presence of the anisotropic JT energy leading to three equivalent minima in the potential surface of each octahedron, corresponding to tetragonal elongations in the x, y, and z directions.

Applying the molecular-field approximation to the coupling terms in Eq. (2) leads to a set of self-consistent equations relating average Pauli matrices of the two sublattices. To achieve this we replace $\sigma_\iota(\vec{n})(\iota = \theta, \epsilon)$ in (2) by their values at each of the three minima. The positions of these minima are negligibly affected by the molecular field near the transition or if the wells are extremely deep:

$$\bar{\sigma}_\theta(-) = \frac{-\exp[B\bar{\sigma}_\theta(+)] + \tfrac{1}{2}\exp\{-B[\tfrac{1}{2}\bar{\sigma}_\theta(+) - \tfrac{1}{2}\sqrt{3}\bar{\sigma}_\epsilon(+)]\} + \tfrac{1}{2}\exp\{-B[\tfrac{1}{2}\bar{\sigma}_\theta(+) + \tfrac{1}{2}\sqrt{3}\bar{\sigma}_\epsilon(+)]\}}{\exp[B\bar{\sigma}_\theta(+)] + \exp\{-B[\tfrac{1}{2}\bar{\sigma}_\theta(+) - \tfrac{1}{2}\sqrt{3}\bar{\sigma}_\epsilon(+)]\} + \exp\{-B[\tfrac{1}{2}\bar{\sigma}_\theta(+) + \tfrac{1}{2}\sqrt{3}\bar{\sigma}_\epsilon(+)]\}},$$

$$\bar{\sigma}_\epsilon(-) = \frac{-\tfrac{1}{2}\sqrt{3}\exp\{-B[\tfrac{1}{2}\bar{\sigma}_\theta(+) - \tfrac{1}{2}\sqrt{3}\bar{\sigma}_\epsilon(+)]\} + \tfrac{1}{2}\sqrt{3}\exp\{-B[\tfrac{1}{2}\bar{\sigma}_\theta(+) + \tfrac{1}{2}\sqrt{3}\bar{\sigma}_\epsilon(+)]\}}{\exp[B\bar{\sigma}_\theta(+)] + \exp\{-B[\tfrac{1}{2}\bar{\sigma}_\theta(+) - \tfrac{1}{2}\sqrt{3}\bar{\sigma}_\epsilon(+)]\} + \exp\{-B[\tfrac{1}{2}\bar{\sigma}_\theta(+) + \tfrac{1}{2}\sqrt{3}\bar{\sigma}_\epsilon(+)]\}}, \tag{3}$$

where

$$B = \frac{[M_c\omega_c^2/(M\omega^2 + 2M_c\omega_c^2)]L^2}{4\hbar\omega kT}.$$

A similar pair of equations exists for $\bar{\sigma}_\theta(+)$ and $\bar{\sigma}_\epsilon(+)$, and can be obtained from Eq. (3) simply by interchanging the (−) and (+) signs labeling the two sublattices.

Written in the polar form, the average Pauli matrices are

$$\bar{\sigma}_\theta(-) = \bar{\sigma}(-)\cos\theta(-), \ldots, \bar{\sigma}_\epsilon(+) = \bar{\sigma}(+)\sin\theta(+).$$

At this point we postulate the following relations between the averages on the two sublattices, which are compatible with the set of equations (3):

$$\bar{\sigma}(+) = \bar{\sigma}(-) \equiv \bar{\sigma}, \quad \theta(+) = n\frac{2\pi}{3} - \theta(-) \equiv \theta, \quad n = 0, \pm 1. \tag{4}$$

The three values of n describe the equivalence of the three main axes. Presumably, the relations given by Eq. (4) are not the only possible ones which solve Eq. (3). However, as will be seen later, they correspond to the observed type of distortion and electronic ordering in most actual examples.

In the following we consider the case with $n = 0$. Having substituted this into Eq. (3) we obtain two coupled transcendental equations for $\bar{\sigma}_\theta(+)$ and $\bar{\sigma}_\epsilon(+)$ or $\bar{\sigma}$ and θ.

In studying the behavior of the static model near the transition point, the expressions in (3) may be expanded near $\bar{\sigma} \sim 0$, where only terms up to the square of $\bar{\sigma}$ are retained. This procedure is justi-

fied in the present case where the transition is of second order, since the order parameter $\bar{\sigma}$ goes smoothly to zero as the transition temperature T_t is approached. [This, however was not the situation in the spinel case (I) where the order parameter still had a finite value at T_t.]

Equations (3) and (4) (with $n=0$) are then written as

$$\bar{\sigma}[\tfrac{1}{8}\bar{\sigma}B^2\cos2\theta+(1+\tfrac{1}{2}B)\cos\theta]=0, \tag{5a}$$

$$\bar{\sigma}[\tfrac{1}{8}\bar{\sigma}B^2\sin2\theta+(1-\tfrac{1}{2}B)\sin\theta]=0. \tag{5b}$$

The solution $\bar{\sigma}=0$ describes the undistorted cubic phase of the perovskite crystal. In order to obtain solutions $\bar{\sigma}\neq 0$, we divide Eq. (5a) by (5b) and have

$$(1+\tfrac{3}{2}B)\cot^2\theta=\tfrac{1}{2}B-1.$$

Since $\cot^2\theta$ is always positive or zero, it is apparent that $\bar{\sigma}$ may differ from zero only if $\frac{1}{2}B>1$, namely,

$$kT\leq\frac{M_c\omega_c^2}{M\omega^2+2M_c\omega_c^2}\frac{L^2}{8\hbar\omega}\equiv kT_t. \tag{6}$$

Equation (6) defines the transition temperature in the static-treatment limit. Defining

$$\lambda\equiv M_c\omega_c^2/M\omega^2$$

and assuming $\lambda\ll 1$, Eq. (6) reduces to $kT_t=\lambda L^2/8\hbar\omega$.

At the transition point $\frac{1}{2}B=1$ and $\cot\theta=0$, i.e., $\theta(+)=-\theta(-)=\frac{1}{2}\pi$. Substituting $\theta=\frac{1}{2}\pi$ into Eq. (5a) gives $\bar{\sigma}=0$ which is characteristic of a second-order phase transition. Further details, concerning the configuration of the ordered phase as well as those arising from the remaining two solutions with $n=\pm 1$, will be discussed in Sec. IV as part of the more general dynamic approach.

III. SOLUTION OF VIBRONIC PROBLEM

When the kinetic energy of the ions is taken into account, the lattice is no longer treated as static and we enter upon the study of the vibronic problem. The ionic displacements appearing in the dynamic JT Hamiltonian must be regarded as quantum-mechanical dynamic variables rather than geometrical parameters.

We use for the E-type vibrational coordinates the same units as in I, namely, write them in a reduced dimensionless form as $q_\theta=Q_\theta(M\omega/\hbar)^{1/2}$, $q_\epsilon=Q_\epsilon(M\omega/\hbar)^{1/2}$, where Q_θ and Q_ϵ are the two normal coordinates of the twofold-degenerate E mode, ω is its frequency, and M is the anionic mass. The mass of the cations is assumed to be sufficiently heavy compared to M, so that their kinetic energy may be neglected.

We lift out of the total Hamiltonian of the crystal the term $H(\vec{n})$ which contains the normal coordinates of the octahedron belonging to the $\vec{n}$th unit cell:

$$H(\vec{n})=\tfrac{1}{2}\hbar\omega\left(-\frac{\partial^2}{\partial q_\theta^2(\vec{n})}-\frac{\partial^2}{\partial q_\epsilon^2(\vec{n})}+q_\theta^2(\vec{n})+q_\epsilon^2(\vec{n})\right)+\tfrac{1}{2}L[q_\theta(\vec{n})\sigma_\theta(\vec{n})+q_\epsilon(\vec{n})\sigma_\epsilon(\vec{n})]$$
$$+\tfrac{1}{4}K[(q_\epsilon^2(\vec{n})-q_\theta^2(\vec{n}))\sigma_\theta(\vec{n})+2q_\theta(\vec{n})q_\epsilon(\vec{n})\sigma_\epsilon(\vec{n})]+\tfrac{1}{4}\sqrt{2}N[3q_\theta(\vec{n})q_\epsilon^2(\vec{n})-q_\theta^3(\vec{n})]+H_{\rm int}, \tag{7}$$

where

$$H_{\rm int}=\tfrac{1}{2}M_c\omega_c^2(\hbar/M\omega)\{[\tfrac{1}{3}\sqrt{3}q_\theta(\vec{n}+\hat{z}a)+\tfrac{1}{3}\sqrt{3}q_\theta(\vec{n})]^2+[-\tfrac{1}{3}\sqrt{3}q_\theta(\vec{n}-\hat{z}a)-\tfrac{1}{3}\sqrt{3}q_\theta(\vec{n})]^2+[\tfrac{1}{2}q_\epsilon(\vec{n}+\hat{x}a)-(1/2\sqrt{3})q_\theta(\vec{n}+\hat{x}a)$$
$$+\tfrac{1}{2}q_\epsilon(\vec{n})-(1/2\sqrt{3})q_\theta(\vec{n})]^2+[-\tfrac{1}{2}q_\epsilon(\vec{n}-\hat{x}a)+(1/2\sqrt{3})q_\theta(\vec{n}-\hat{x}a)-\tfrac{1}{2}q_\epsilon(\vec{n})+(1/2\sqrt{3})q_\theta(\vec{n})]^2$$
$$+[-\tfrac{1}{2}q_\epsilon(\vec{n}+\hat{y}a)-(1/2\sqrt{3})q_\theta(\vec{n}+\hat{y}a)-\tfrac{1}{2}q_\epsilon(\vec{n})-(1/2\sqrt{3})q_\theta(\vec{n})]^2$$
$$+[\tfrac{1}{2}q_\epsilon(\vec{n}-\hat{y}a)+(1/2\sqrt{3})q_\theta(\vec{n}-\hat{y}a)+\tfrac{1}{2}q_\epsilon(\vec{n})+(1/2\sqrt{3})q_\theta(\vec{n})]^2\}.$$

$H_{\rm int}$ is the elastic energy due to interaction between the B-site cations, expressed in terms of the normal displacements of the nearest set of octahedra.

L, K, and N are the coefficients of the vibronic coupling terms which are linear, quadratic, and cubic in the vibrational coordinates, respectively. These coupling coefficients have all the same dimension (energy) and are given in terms of the derivatives of the electronic potential V by

$$L=-\left\langle E_\theta\left|\frac{\partial V}{\partial q_\theta}\right|E_\theta\right\rangle+\left\langle E_\epsilon\left|\frac{\partial V}{\partial q_\theta}\right|E_\epsilon\right\rangle,$$

$$K=\left\langle E_\theta\left|\frac{\partial^2 V}{\partial q_\theta^2}\right|E_\theta\right\rangle-\left\langle E_\epsilon\left|\frac{\partial^2 V}{\partial q_\theta^2}\right|E_\epsilon\right\rangle,$$

$$M=-\tfrac{1}{6}\sqrt{2}\left(\left\langle E_\theta\left|\frac{\partial^3 V}{\partial q_\theta^3}\right|E_\theta\right\rangle+\left\langle E_\epsilon\left|\frac{\partial^3 V}{\partial q_\theta^3}\right|E_\epsilon\right\rangle\right).$$

In applying the molecular-field-approximation method to the Hamiltonian of Eq. (7), all the normal displacements q_θ, q_ϵ other than those belonging to the $\vec{n}$th unit cell are replaced by their average values $\bar{q}_\theta$ and $\bar{q}_\epsilon$. Following the discussion in the static treatment of Sec. II, we assume the existence of two sublattices and replace $q_\theta(\vec{n}')$ and $q_\epsilon(\vec{n}')$ in $H(\vec{n})$ $(\vec{n}'\neq\vec{n})$ by $\bar{q}_\theta(-)$ and $\bar{q}_\epsilon(-)$, respectively, where the averages are defined by

$$\bar{q}_\iota(-)=\mathrm{Tr}\,[q_\iota(\vec{n}')e^{-H(\vec{n}')/kT}]/\mathrm{Tr}\,e^{-H(\vec{n}')/kT}$$

$$(\iota=\theta,\epsilon),\ \text{etc.}\qquad(8)$$

The self-consistency which the set of Eqs. (8) introduce into the formalism is apparent since $H(\vec{n}')$ is itself a function of $\bar{q}_\iota(+)$. We write $q_\theta(\vec{n}')=\bar{q}_\theta(-)+[q_\theta(\vec{n}')-\bar{q}_\theta(-)]$ and regard the second term as small so that the square can be neglected. Now lumping together into $H(\vec{n})$ only those terms which do not depend on $\vec{n}'$, H_{int} of Eq. (7) becomes

$$\lambda\hbar\omega[q_\theta(\vec{n})\bar{q}_\theta(-)+q_\epsilon(\vec{n})\bar{q}_\epsilon(-)-\bar{q}_\theta(+)\bar{q}_\theta(-)-\bar{q}_\epsilon(+)\bar{q}_\epsilon(-)],\qquad(9)$$

where λ has already been defined in the static treatment as

$$\lambda\equiv M_c\omega_c^2/M\omega^2.$$

Under conditions of strong linear JT coupling, i.e., $L/\hbar\omega\gg1$, the Hamiltonian given by Eqs. (7) and (9) can be approximately diagonalized in a way similar to the single-center case.[16-19] This is achieved by transforming to a new set:

$$|\psi_-\rangle=\cos\tfrac{1}{2}\varphi\,|E_\theta\rangle-\sin\tfrac{1}{2}\varphi\,|E_\epsilon\rangle,$$

$$|\psi_+\rangle=\sin\tfrac{1}{2}\varphi\,|E_\theta\rangle+\cos\tfrac{1}{2}\varphi\,|E_\epsilon\rangle,$$

where φ is the angle in the polar form of the vibrational coordinates[20]

$$q_\theta=q\cos\varphi,\quad q_\epsilon=q\sin\varphi.$$

Assuming a deep radial potential and restricting q to its mean value $q_0\sim L/2\hbar\omega$, the problem reduces to that of solving the angular Schrödinger equation

$$H(+)\chi(\varphi)=\left(-\alpha\frac{\partial^2}{\partial\varphi^2}-\beta\cos3\varphi+\gamma_\theta'(-)\cos\varphi+\gamma_\epsilon'(-)\sin\varphi\right.$$
$$\left.-(\lambda\hbar\omega q_0^2)^{-1}[\gamma_\theta'(-)\gamma_\theta'(+)+\gamma_\epsilon'(-)\gamma_\epsilon'(+)]\right)\chi(\varphi)=E\chi(\varphi).\qquad(10)$$

Here

$$\alpha=\hbar\omega/2q_0^2,\quad\beta=\tfrac{1}{4}\sqrt{2}\,Nq_0^3-\tfrac{1}{4}Kq_0^2,$$
$$\gamma_\iota'(\mp)=+\lambda\hbar\omega q_0\bar{q}_\iota(\mp)\qquad(\iota=\theta,\epsilon).\qquad(11)$$

Note that the definition of $\gamma_\theta'(\mp)$ is identical to that of γ_θ in the spinel case [see Eq. (11) of I]. However, the sign with which γ_θ appeared in the angular Hamiltonian of the spinel was negative [I, Eq. (10)]. It has already been noted that for d^4 and d^9 ions at octahedral sites, $\beta>0$.

The state of the system in each sublattice is given by the solution of Eq. (10), and is dependent on the temperature through the presence of γ_θ' and γ_ϵ' in the Hamiltonian. As will be shown in Sec. IV, a temperature T_t exists, above which both γ_θ' and γ_ϵ' of the two sublattices vanish, corresponding to the cubic phase of the crystal. Below T_t, nonzero solutions for γ_θ' and γ_ϵ' exist and the stable state of the system is that of a distorted crystal.

The eigenvalues and eigenfunctions of Eq. (10) are found by numerical matrix diagonalization subject to setting the parameters γ_θ' and γ_ϵ' equal to what is obtained self-consistently from Eq. (8).

In the spinel problem γ_ϵ was equal to zero because of symmetry considerations, so that the angular Hamiltonian became an even function of φ. This made possible the reduction of the Hamiltonian matrix to a direct sum in the even and odd representations (see Appendix of I). In the present case, one can not put $\gamma_\epsilon'=0$ without a simultaneous vanishing of γ_θ' so that a similar matrix reduction cannot be performed.

In the limit of $\beta/\alpha\gg1$, the three lowest vibronic states alone may be retained, corresponding to what we have called (I, Sec. III) the three-state approximation. The matrix of the Hamiltonian of Eq. (10) in the representation of $|\Psi_\theta\rangle$, $|\Psi_\epsilon\rangle$ and $|\Psi_{A_1}\rangle$, which are the lowest doublet and adjacent singlet of the cubic Hamiltonian, is

$$\begin{array}{c|}|\Psi_\theta\rangle\\|\Psi_\epsilon\rangle\\|\Psi_{A_1}\rangle\end{array}\begin{bmatrix}q\gamma_\theta'(-) & -q\gamma_\epsilon'(-) & -r\gamma_\theta'(-)\\ q\gamma_\epsilon'(-) & -q\gamma_\theta'(-) & -r\gamma_\epsilon'(-)\\ -r\gamma_\theta'(-) & -r\gamma_\epsilon'(-) & 3\Gamma\end{bmatrix}+E_E-\frac{[\gamma_\theta'(-)\gamma_\theta'(+)+\gamma_\epsilon'(-)\gamma_\epsilon'(+)]}{\lambda\hbar\omega q_0^2}.\qquad(12)$$

Here E_E is the energy of the lowest vibronic doublet of the cubic angular Hamiltonian

$$E_E = \alpha\nu - 4\nu^2\pi^2\alpha\gamma/[9(1+\gamma)] + 8\nu^2 e^{-9/8\nu}\alpha(1-\gamma)/[9(1+\gamma)],$$

where $\nu \equiv (9\beta/8\alpha)^{1/2}$ and $\gamma \equiv e^{-2\nu\pi^2/9}$. The energy difference between this doublet and the adjacent singlet is

$$3\Gamma = 3\beta\gamma[\tfrac{1}{2}\pi^2(1+\gamma) - 2e^{-9/8\nu}].$$

The parameters q and r are Ham's reduction factors.[18] In the three-state approximation they are

$$q = \tfrac{1}{2}e^{-1/8\nu}(1+2\gamma)/(1+\gamma),$$

$$r = -\tfrac{1}{2}\sqrt{2}\, e^{-1/8\nu}(1-\gamma)/[(1+\gamma)(1-2\gamma)]^{1/2}.$$

Being interested in the solutions in the vicinity of T_t, we are allowed to regard γ_θ' and γ_ϵ' in Eq. (12) as small perturbations, since the transition is of the second order. We write γ_θ' and γ_ϵ' in the polar form

$$\gamma_\theta'(\pm) = \mu(\pm)\cos\theta(\pm), \quad \gamma_\epsilon'(\pm) = \mu(\pm)\sin\theta(\pm). \tag{13}$$

It is obvious that $\mu(\pm) = -\lambda\hbar\omega q_0^2\bar{\sigma}(\pm)$, where $\bar{\sigma}$ is defined in Sec. II. (For the minus sign see Ref. 20.) Omitting the (−) label of the second sublattice and assuming $\mu \ll 3\Gamma$, we obtain the following expressions for the eigenvalues of the matrix in Eq. (12) and expectation values, correct to second order in μ:

$$\begin{pmatrix} E_1 \\ E_2 \end{pmatrix} = \pm\mu q - \tfrac{1}{2}\mu^2 r^2(1 \pm \cos3\theta)/3\Gamma,$$

$$E_3 = 3\Gamma + \mu^2 r^2/3\Gamma,$$

$$\begin{pmatrix} \langle\Psi_1|\cos\varphi|\Psi_1\rangle \\ \langle\Psi_2|\cos\varphi|\Psi_2\rangle \end{pmatrix} = \pm q\cos\theta \mp \tfrac{1}{2}r^2(\mu/3\Gamma)(\sin\theta\sin3\theta + 2\cos2\theta \pm 2\cos\theta) \mp \tfrac{1}{2}r^2(\mu/3\Gamma)^2[\sin3\theta(2\sin2\theta + 3\cos\theta\sin3\theta)r^2/4q + 3q(\cos\theta \pm \cos2\theta)],$$

$$\langle\Psi_3|\cos\varphi|\Psi_3\rangle = 2r^2(\mu/3\Gamma)\cos\theta + 3r^2q(\mu/3\Gamma)^2\cos2\theta, \tag{14}$$

$$\begin{pmatrix} \langle\Psi_1|\sin\varphi|\Psi_1\rangle \\ \langle\Psi_2|\sin\varphi|\Psi_2\rangle \end{pmatrix} = \pm q\sin\theta \pm \tfrac{1}{2}r^2(\mu/3\Gamma)(\cos\theta\sin3\theta + 2\sin2\theta \mp 2\sin\theta) \pm \tfrac{1}{2}r^2(\mu/3\Gamma)^2[\sin3\theta(\cos2\theta + \cos\theta\cos3\theta 3r^2/4q) + 3q(\sin2\theta \mp \sin\theta)],$$

$$\langle\Psi_3|\sin\varphi|\Psi_3\rangle = 2r^2(\mu/3\Gamma)\sin\theta - 3r^2q(\mu/3\Gamma)^2\sin2\theta.$$

We shall use these results in Sec. IV.

IV. ANALYSIS OF CRITICAL REGION AND LOW-TEMPERATURE CONFIGURATION

In dealing with a two-sublattice system it is reasonable to define a free-energy function F for an assembly of octahedra with a Hamiltonian which is the sum of $H(+)$ and $H(-)$ of Eq. (10). However, the term

$$-(\lambda\hbar\omega q_0^2)^{-1}[\gamma_\theta'(-)\gamma_\theta'(+) + \gamma_\epsilon'(-)\gamma_\epsilon'(+)]$$

expressing the mean interaction between neighboring octahedra is equally felt by each of the sublattices and, therefore, should obviously appear only once in the expression for F.

In thermal equilibrium each of the four derivatives of F with respect to $\gamma_\iota'(\pm)$ ($\iota = \theta, \epsilon$) must be equal to zero. This results in obtaining four self-consistent equations, which are

$$\frac{1}{\lambda\hbar\omega q_0^2}\begin{pmatrix} \gamma_\theta'(\pm) \\ \gamma_\epsilon'(\pm) \end{pmatrix} = \mathrm{Tr}\begin{pmatrix} \cos\varphi \\ \sin\varphi \end{pmatrix} e^{-H(\pm)/kT} \Big/ \mathrm{Tr}\, e^{-H(\pm)/kT}. \tag{15}$$

The equivalence of Eqs. (15) and (8) is immediate. In addition, the second derivatives of F must be positive. This can be ensured by adding to the free-energy quadratic terms of the form

$$(\gamma_\theta' - \lambda\hbar\omega q_0^2\langle\cos\varphi\rangle)^2 + (\gamma_\epsilon' - \lambda\hbar\omega q_0^2\langle\sin\varphi\rangle)^2,$$

where the averages $\langle\cdots\rangle$ are calculated at equilibrium. We have no microscopic Hamiltonian which yields these quadratic terms; however, these terms do not alter Eq. (15), whose validity is anchored to the self-consistency conditions [Eq. (8)] independently of the free energy.

Equations (15) must be invariant under a change in the sign of the integration variable φ. Having performed such a transformation in, e.g., the equation for the (+) sublattice, and then replacing $\gamma_\theta'(-)$ by $\gamma_\theta'(+)$ and $\gamma_\epsilon'(-)$ by $-\gamma_\epsilon'(+)$ throughout, one obtains the equation for the (−) sublattice, and vice versa. This solution corresponds to Eq. (4) with $n=0$. The two other solutions of Eq. (4), namely, $\theta(-)=\frac{2}{3}\pi-\theta(+)$ and $\theta(-)=-\frac{2}{3}\pi-\theta(+)$, can be shown to solve Eq. (15) as well. Note that each of the solutions in Eq. (4) leaves the two sublattices energetically equivalent.

For small and moderate values of β/α, numerical methods involving multidimensional matrix diagonalization were applied in order to solve Eqs. (15). However, for high values of β/α, it is possible to take advantage of the analytical expressions for the eigenvalues and expectation values in the three-state approximation, Eq. (14). Assuming $\mu \ll 3\Gamma \ll kT$ and defining

$$\theta(+)=-\theta(-)\equiv\theta, \quad \mu(+)=\mu(-)\equiv\mu,$$

we obtain

$$\mu\left\{\mu\lambda\hbar\omega q_0^2\frac{r^2 q}{(kT)^2}\left(\frac{1}{2}+\frac{\Gamma}{kT}\right)\cos 2\theta-\frac{2}{3}\frac{\lambda\hbar\omega q_0^2}{kT}\left[q^2\left(1+\frac{3\Gamma}{kT}\right)+r^2\left(1+\frac{3\Gamma}{2kT}\right)\right]\cos\theta-\left(1+\frac{2\Gamma}{kT}\right)\cos\theta\right\}=0, \tag{16a}$$

$$\mu\left\{\mu\lambda\hbar\omega q_0^2\frac{r^2 q}{(kT)^2}\left(\frac{1}{2}+\frac{\Gamma}{kT}\right)\sin 2\theta+\frac{2}{3}\frac{\lambda\hbar\omega q_0^2}{kT}\left[q^2\left(1+\frac{3\Gamma}{kT}\right)+r^2\left(1+\frac{3\Gamma}{2kT}\right)\right]\sin\theta-\left(1+\frac{2\Gamma}{kT}\right)\sin\theta\right\}=0. \tag{16b}$$

Looking for a solution $\mu\neq 0$ we arrive at the equation

$$\cot^2\theta\left\{1+\frac{2\lambda\hbar\omega q_0^2}{kT}\left[q^2\left(1+\frac{\Gamma}{kT}\right)+r^2\left(1-\frac{\Gamma}{2kT}\right)\right]\right\}=\frac{2}{3}\frac{\lambda\hbar\omega q_0^2}{kT}\left[q^2\left(1+\frac{\Gamma}{kT}\right)+r^2\left(1-\frac{\Gamma}{2kT}\right)\right]-1,$$

which has solutions only if its right-hand side is greater or equal to zero; thus

$$T\leq\tfrac{1}{3}(\lambda\hbar\omega q_0^2/k)\{(q^2+r^2)+[(q^2+r^2)^2+(3\Gamma/\lambda\hbar\omega q_0^2)(2q^2-r^2)]^{1/2}\}\equiv T_t. \tag{17}$$

For large values of β/α, $q\to\frac{1}{2}$, $r\to\frac{1}{2}\sqrt{2}$, and $3\Gamma\to 0$, so that the transition temperature of Eq. (17) becomes $kT_t=\frac{1}{2}\lambda\hbar\omega q_0^2$. Substituting for q_0 its ground-state value, i.e., $q_0\sim L/2\hbar\omega$, it is obvious that this expression for the transition temperature coincides with the static-treatment result of Sec. II, provided that $\lambda\ll 1$.

It is interesting to analyse the behavior of the order parameters γ_θ' and γ_ϵ', or μ and θ just below the transition point. At the transition temperature $\cot\theta=0$, θ is equal to $\frac{1}{2}\pi$ and substituting this in Eq. (16a), $\mu=0$. When the temperature is slightly decreased the following inequalities arise after multiplying Eq. (16a) by $\cos\theta$ and (16b) by $\sin\theta$:

$$\mu\cos 2\theta\cos\theta>0, \quad \mu\sin 2\theta\sin\theta<0. \tag{18}$$

From the second inequality we have $\mu\cos\theta<0$, which means that γ_θ' and, more importantly, the mean tetragonal distortion $\bar{q}_\theta$ of both sublattices are negative [see Eq. (11)].

Following Kanamori,[3] we represent the sublattice mean distortions as vectors in the $\bar{q}_\theta, \bar{q}_\epsilon$ plane (see Fig. 2). In the vicinity of T_t the two vectors are almost antiparallel to each other in the direction of the $\bar{q}_\epsilon$ axis, but both are slightly canted towards the negative $\bar{q}_\theta$ axis [drawn by full lines in Fig. 2(a)]. The canting angle vanishes at the transition point ($\theta=\frac{1}{2}\pi$)[drawn by dotted lines in Fig. 2(a)], and increases with decreasing the temperature. Thus, on the average, the two sublattices exhibit opposite orthorhombic distortion amplitudes $\bar{q}_\epsilon$ but both have negative tetragonal distortions $\bar{q}_\theta$. Consequently, three unequal transition-metal–oxygen distances are formed in the ordered phase, the short and long ones alternating along the x and y directions, and the distance along the z direction being in between them.

This corresponds to a tetragonal distortion of the pseudo-unit-cell along the z axis with $c_0/a_0<1$. However, the true crystallographic cell of the ordered phase, which contains four distorted perovskite units, is tetragonal with $c/a>1$. Here $c=2c_0$ and $a=\sqrt{2}a_0$, where c_0 and a_0 designate the lattice constants of the pseudocell.

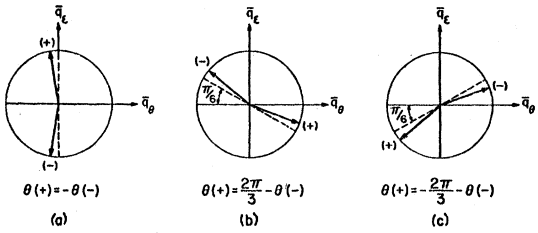

FIG. 2. Sublattice distortion in the $\bar{q}_\theta$, $\bar{q}_\epsilon$ plane for the perovskite structure, where the tetragonal axis of the unit cell is (a) along the Z direction and (b) and (c) along the Y and X directions. Broken lines and heavy-line arrows represent the configuration at, and somewhat below, the transition temperature, respectively.

X-ray diffraction patterns of, e.g., $KCuF_3$, indicate the existence of three different metal-fluorine bonds and show the displacements of F^- ions in successive (001) planes to be in opposite directions.[7,8] This structure coincides with the type of ordering which arises from the above-discussed model, where we have chosen the relation between the two sublattices to be given by Eq. (4).

Although this type of ordering is the most common one, there is evidence to the existence of another type,[7] in which the F^- displacements in successive (001) planes are in the same direction. This distortion, as well as the completely ferrodistortive one suggested by Blasse[13] for A_2CuWO_6 (A = Sr, Ba) are not discussed by us.

Solving Eqs. (16) for $T < T_t$ and taking $\Gamma/kT \ll 1$, $2q^2 \sim r^2$ gives

$$\mu \approx 4kT(T_t - T)^{1/2}/T_t^{1/2} ,$$

$$\cos\theta \approx -\tfrac{1}{2}(T_t - T)^{1/2}/T_t^{1/2} ,$$

$$\sin\theta \approx \tfrac{1}{2}(3T_t + T)^{1/2}/T_t^{1/2} .$$

Thus in the critical region below T_t the temperature dependence of the mean distortions is given by

$$\bar{q}_\theta(+) = \bar{q}_\theta(-) \propto T_t - T ,$$
$$\bar{q}_\epsilon(+) = -\bar{q}_\epsilon(-) \propto (T_t - T)^{1/2} . \qquad (19)$$

The square-root law of $\bar{q}_\epsilon$ is typical of a second-order phase transition. The critical-region behavior of Eq. (19) can be seen in the extreme right-hand side of Fig. 3. In this figure, results of the numerical solution of Eqs. (15) are displayed for some typical values of the parameters.

Sugawara *et al.*[12] investigated the crystallographic phase transitions occurring in $BiCrO_3$ and $BiMnO_3$ crystals. In $BiCrO_3$, which should exhibit no cooperative JT distortion since it contains a nondegenerate cation, they found a thermal hysteresis of the magnetic susceptibility associated with a noticeable two-phase region, which is characteristic of a first-order transition. Although the distortion of $BiMnO_3$ exceeded that in $BiCrO_3$, no thermal hysteresis was observed in the former. This lends support to the second-order nature of the JT-induced transition.

In order to study the low-temperature configuration, we have plotted the canting angle of the sublattice distortion at 0 °K as a function of the molecular-field strength, for two values of β/α (Fig. 4). As β/α decreases, θ becomes closer to $\frac{1}{2}\pi$ which can be shown to be the solution of Eq. (15) when β vanishes. $\frac{1}{2}\pi$ is also the limiting value for θ shown on the extreme right of the figure, when β becomes negligible with respect to the

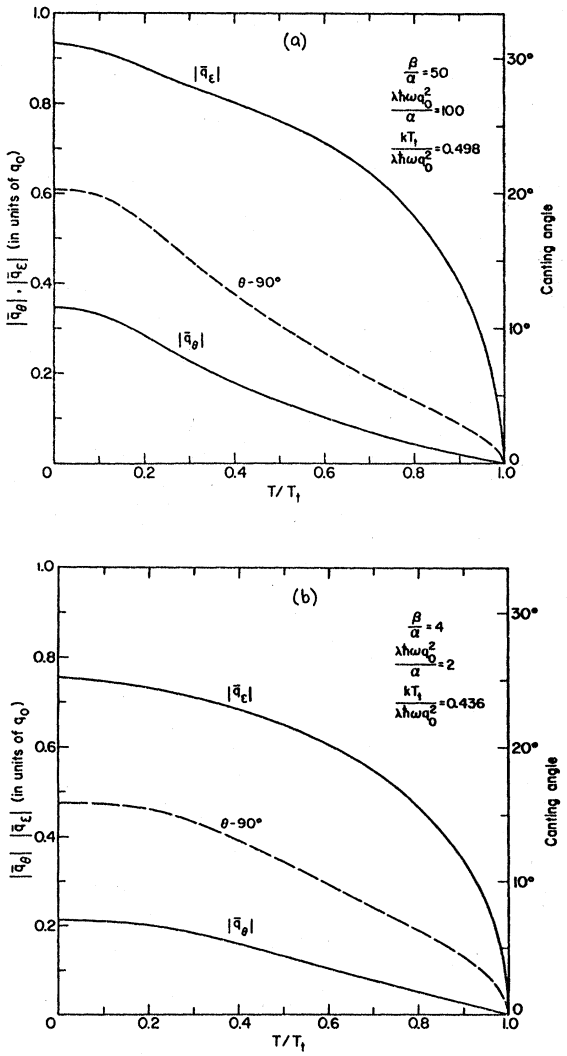

FIG. 3. Mean normal coordinates and canting angle of sublattice distortion, (a) for high and (b) for low molecular-field and anisotropy energies.

molecular-field strength. The limiting value of θ on the left end of Fig. 4 corresponds to zero molecular field and is compatible with the value $\theta = \frac{1}{2}\pi$ at the transition point. Referring to Eqs. (3) of the static extremely anisotropic treatment, it can be shown that at very low temperatures

$$\overline{\sigma}_\theta(+) = \overline{\sigma}_\theta(-) \to \tfrac{1}{2}\,,$$

$$\overline{\sigma}_\epsilon(+) = -\overline{\sigma}_\epsilon(-) \to \tfrac{1}{2}\sqrt{3},$$

so that $\theta = \theta(+) \to \frac{2}{3}\pi$, $\theta(-) \to -\frac{2}{3}\pi$ provided that

$$\lim[(\tfrac{2}{3}\pi - \theta)/T] \to \infty \text{ as } T \to 0.$$

This is displayed by the horizontal dotted line at $\theta = \frac{2}{3}\pi$ in Fig. 4. This limit corresponds to a configuration in which each single complex is tetragonally elongated along the x and y axes, alternatively. The pseudo-unit-cell undergoes a tetragonal distortion with $c/a < 1$.

Calculated specific-heat curves vs temperature are displayed in Fig. 5. A similar low-temperature anomalous hump was experimentally observed by Bokov *et al.*[5] in some manganite systems. However, they interpret this behavior as associated with an antiferromagnetic transition occurring at low temperatures. Sharp humps were earlier reported in the specific-heat curves of KMF_3 (M = Cu, Co, and the nondegenerate Ni^{2+}).[11]

V. TRANSITION TEMPERATURE

Figure 6 shows curves of the reduced transition temperature with different values of β/α. The abscissa is the ratio of the molecular-field strength $\lambda\hbar\omega q_0^2$ to $(\alpha\beta)^{1/2}$. In the limit $\beta/\alpha \to \infty$, the lowest vibronic energy levels of the cubic angular Hamiltonian $-\alpha(\partial^2/\partial\varphi^2) - \beta\cos 3\varphi$ are approximately given by $-\beta + 3(2n+1)(\frac{1}{2}\alpha\beta)^{1/2}$, $(n = 0, 1, \cdots)$, and are threefold nearly degenerate. Thus, $3(2\alpha\beta)^{1/2}$ gives the energy separation between the set of the three lowest vibronic states and the higher-lying states.

In the following we discuss the variation of the transition temperature referring to the same five regimes which have been introduced in I.

(a) Starting with extremely high values of β/α, provided that

$$3\Gamma \ll \lambda\hbar\omega q_0^2 \ll (\alpha\beta)^{1/2}\,,$$

we may apply the static limit treatment where we have found $kT_t/\lambda\hbar\omega q_0^2 = \frac{1}{2}$. [See Eq. (6) with $M_c\omega_c^2 \ll M\omega^2$ and $q_0 = L/2\hbar\omega$.]

(b) For moderately high values of β/α, where

$$3\Gamma \sim \lambda\hbar\omega q_0^2 \ll (\alpha\beta)^{1/2}\,,$$

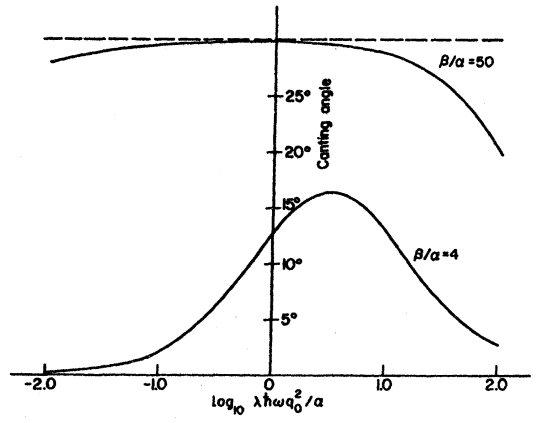

FIG. 4. Canting angle of sublattice distortion at 0 °K as function of the molecular-field strength for $\beta/\alpha = 4$ and 50. Broken line represents the static extremely anisotropic behavior.

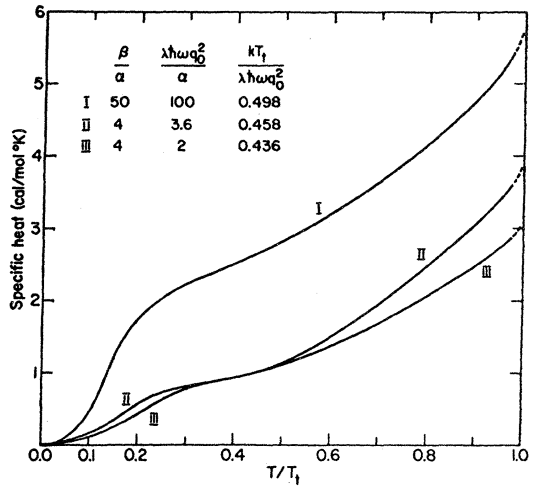

FIG. 5. Temperature dependence of the specific heat for values of the physical parameters shown in the first two columns in the inset.

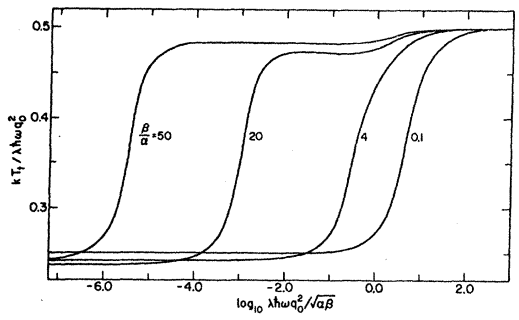

FIG. 6. Reduced transition temperature as function of the molecular-field strength plotted for different strengths of the nonlinear coupling. (These curves may be compared to those in Fig. 9 of Ref. 1.)

the three-state approximation, Eq. (12), is valid, leading to reduced T_t somewhat below 0.5 [Eq. (17)].

(c) The intermediate region covering values between 0.5 down to almost 0.25 belongs to what we have called the general regime. This includes $\beta \gg \alpha$ as well as $\beta \leq \alpha$, provided that the molecular field is sufficiently strong to cause excitations into several high-lying vibronic states.

(d) The right-hand extreme of Fig. 6 corresponds to the strong molecular-field limit, i.e., $\lambda\hbar\omega q_0^2 \gg \alpha, \beta$, where the reduced transition temperature approaches the value $\frac{1}{2}$.

The analytical derivation of this limiting value is as following: Near the transition point, $\gamma_\theta' \ll \gamma_\epsilon'$, so that we may neglect the term $\gamma_\theta' \cos\varphi$ in the Hamiltonian of Eq. (10) and write

$$H(+) = -\alpha\partial^2/\partial\varphi^2 - \beta\cos 3\varphi + \gamma_\epsilon'(-)\sin\varphi \ ,$$

ignoring constant terms which do not enter the expressions for thermal averages. We define

$$H_0(+) = -\frac{\alpha\partial^2}{\partial\varphi^2} - \beta\cos 3\varphi$$

and put $\gamma_\epsilon'(-) = -\gamma_\epsilon'(+)$. If we now omit the (+) sign labeling the sublattice and write γ_ϵ' instead of $\gamma_\epsilon'(+)$, we have for the commutation relation

$$[H, H_0] = +\gamma_\epsilon' \cdot \alpha\left(\sin\varphi - 2\cos\varphi\frac{\partial}{\partial\varphi}\right)$$

Assuming $\alpha, \beta, \gamma_\epsilon' \ll kT$, appropriate for the strong molecular-field case since kT_t is of the order of $\lambda\hbar\omega q_0^2$, using the operational expansion

$$e^A \cdot e^B = e^{A+B+(1/2)[A,B]+(1/12)[[A,B],B]+(1/12)[[B,A],A]+\cdots} ,$$

and neglecting terms of order $1/(kT)^2$, we have

$$e^{-H/kT} = (1 + \gamma_\epsilon' \sin\varphi/kT + \cdots)\, e^{-H_0/kT} \ .$$

Substituting into the self-consistent equation [Eq. (15)], we obtain

$$\gamma_\epsilon'/\lambda\hbar\omega q_0^2 = \frac{\mathrm{Tr}(\sin\varphi + \gamma_\epsilon' \sin^2\varphi/kT + \cdots)\, e^{-H_0/kT}}{\mathrm{Tr}(1 + \gamma_\epsilon' \sin\varphi/kT + \cdots) e^{-H_0/kT}} \ . \tag{20}$$

From symmetry arguments it is easy to verify that Tr $\sin\varphi\, e^{-H_0/kT}$ as well as Tr $\cos 2\varphi\, e^{-H_0/kT}$ vanish. Having written $\sin^2\varphi$ as $\frac{1}{2} - \frac{1}{2}\cos 2\varphi$ and equating the coefficients of γ_ϵ' on both sides of Eq. (20), we obtain

$$kT_t/\lambda\hbar\omega q_0^2 = \tfrac{1}{2} \ .$$

(e) The left-hand extreme of Fig. 6 corresponds to what we have called the "Ising-model limit." Here the molecular-field strength is much smaller than the separation between the doublet and singlet, so that only the two lowest states need to be considered. The limiting self-consistent equation is of the form

$$\mu/\lambda\hbar\omega q_0^2 = q\tanh(\mu q/kT)$$

and the reduced transition temperature approaches the value q^2, where q is Ham's reduction factor.[18]

The dependence of $\langle\cos\varphi\rangle$ on the molecular-field strength for constant temperature is shown in Fig. 7. Attention is directed to the implicit dependence of the molecular field on the JT ion concentration. Although our theory was developed for full concentration $x = 1$, it is obvious that for $0 < x < 1$ the quantity $\lambda\hbar\omega q_0^2$ should get multiplied by x, which calls for a new definition of λ as λx. Thus Fig. 7 displays the effect of reduction of the JT ion concentration on the axial distortion and shows the existence of a critical concentration, corresponding to the abscissa taking the value ~ 2.3, below which $\langle\cos\varphi\rangle$ vanishes and the distortion disappears. A critical concentration $x \sim 0.8$ was experimentally established in $La(Mn^{3+} - Mn^{4+})O_3$ systems.[6] A linear dependence on x was found in some mixed perovskites.[15] Our model does not apply to these.

The axial ratio of the true crystallographic cell (containing four perovskite units) is given by

$$c/a = \sqrt{2}[1 + \langle\cos\varphi\rangle\sqrt{3}/(l_0/Q_0 - \langle\cos\varphi\rangle/\sqrt{3})]$$

$$(\langle\cos\varphi\rangle < 0) \ ,$$

where l_0 is the length of the undistorted octahedral axis. Taking as typical value $Q_0/l_0 = 0.075$, one gets a saturation value of $c/a = 1.381$ for the system described in Fig. 7. As was shown by Kanamori,[3] the ratio $\bar{q}_\theta/\bar{q}_\epsilon$ can be expressed in terms of the three Mn-O distances observed in the tetragonally distorted phase, giving

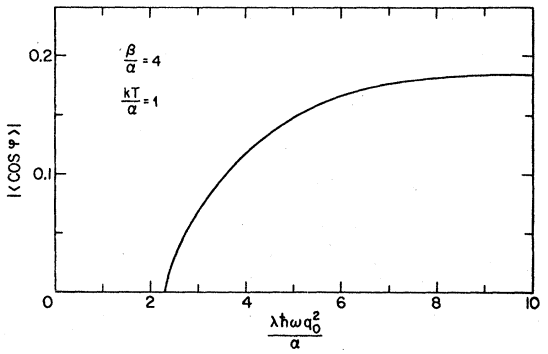

FIG. 7. The thermal average $\langle\cos\varphi\rangle$ (equal to $\bar{q}_\theta/q_0$) as function of the molecular-field strength in a perovskite, drawn for a fixed temperature.

$$\bar{q}_\theta(\pm)/\bar{q}_\epsilon(\pm) = \cot\theta(\pm) = \pm(2m - l - s)/\sqrt{3}(l - s), \quad (21)$$

where l and s stand for the long and short distances alternating along the x and y directions, and m is the Mn-O distance along the z axis.

X-ray measurements of the three different distances in MnF_3 perovskites[8] give $l = 2.09$ Å, $m = 1.91$ Å, and $s = 1.79$ Å, yielding a rather small canting angle of 6 deg 35 min. On the other hand, the copper-fluorine distances in $KCuF_3$ crystals[7] are found to be $l = 2.25$ Å, $m = 1.96$ Å, and $s = 1.89$ Å, corresponding to a canting angle of 19 deg 24 min.[21]

From the observed transition temperatures in perovskites which are about a few hundreds of degrees[4,6] the molecular-field strength $\lambda\hbar\omega q_0^2$ is possibly about 10^3 cm^{-1}.

Taking $\alpha \sim 10$ cm^{-1} and $\beta \sim 500$ cm^{-1}, we see from Fig. 4 that the maximal canting angle amounts to 20°, which is close to the observed value in $KCuF_3$. The small canting angle in MnF_3 corresponds to much smaller values of β which, referring to Fig. 4, are estimated as lower than 100 cm^{-1}.

VI. CONCLUSIONS

The theory presented for antiferrodistortive perovskites follows Kanamori's theory in physical content, but has been made more tangible (by the use of a specific though restricted model), more realistic (by the inclusion of the dynamic effect), and more quantitative (thereby becoming comparable with experiment). We recall the curves of the rather unusual specific heat as functions of temperature (Fig. 5) and the distortion-vs-JT-ion concentration. The transition is of the second order, appropriate to a two-sublattice system. It was seen to vary between one-quarter and one-half of the molecular-field energy (Fig. 6) almost as for spinels (I). In the canting angle of the sublattice distortion [Eq. (21)] a new measurable quantity appears[3] for perovskites which depends upon most of the physical parameters and is relatively easily accessible to experiment. Its limiting zero-temperature value is small than $\frac{2}{3}\pi$, its value for extremely strong anisotropic energy.[3]

The main limitations on the validity of the theory are similar to those in Paper I and were discussed there: the use of the molecular or mean field approximation, the exclusive attention paid to the angular distortion (in the q_θ, q_ϵ plane), and the assumption of infinitely heavy (though not rigidly fixed) cations. The restriction in the type of distortion imposed by Eq. (4) is also recalled.

---

[1]R. Englman and B. Halperin, Phys. Rev. B 2, 75 (1970).

[2]J. B. Goodenough, *Magnetism and the Chemical Bond* (Interscience, New York, 1963).

[3]J. Kanamori, J. Appl. Phys. 31, 14S (1960).

[4]E. E. Havinga, Philips Res. Rept. 21, 432 (1966).

[5]V. A. Bokov, N. A. Grigoryan, M. F. Bryzhina, and V. V. Tikhonov, Phys. Status Solidi 28, 835 (1968).

[6]A. Wold and R. J. Arnott, J. Phys. Chem. Solids 9, 176 (1959).

[7]A. Okazaki, Y. Suemune, and T. Fuchikami, J. Phys. Soc. Japan 14, 1823 (1959); A. Okazaki and Y. Suemune, *ibid.* 16, 176 (1961).

[8]H. A. Hepworth and K. H. Jack. Acta Cryst. 10, 345 (1957).

[9]A. J. Edwards and R. D. Peacock, J. Chem. Soc. (London) 4, 4126 (1959).

[10]K. Knox, Acta. Cryst. 14, 583 (1961).

[11]K. Hirakawa, K. Hirakawa, and T. Hashimoto, J. Phys. Soc. Japan 15, 2063 (1960).

[12]F. Sugawara, S. Iida, Y. Syono, and S. Akimoto, J. Phys. Soc. Japan 25, 6 (1968).

[13]G. Blasse, Philips Res. Rept. 20, 327 (1965).

[14]M. Marsh and C. C. Clark, Phil. Mag. 19, 449 (1969).

[15]D. Reinen, Z. Naturoforsch. 23a, 521 (1968); C. Friebel and D. Reinen, *ibid.* 24a, 1518 (1969).

[16]M. C. M. O'Brien, Proc. Roy. Soc. (London) A281, 323 (1964).

[17]K. A. Müller, in *Magnetic Resonance and Relaxation*, edited by R. Blinc (North-Holland, Amsterdam, 1967), p. 192.

[18]F. S. Ham, in *Electron Paramagnetic Resonance*, edited by S. Geschwind (Plenum, New York, 1970).

[19]M. D. Sturge, in *The Jahn-Teller Effect in Solids*, *Solid State Physics*, edited by F. Seitz, D. Turnbull, and H. Ehrenreich (Academic, New York, 1967), Vol. 20.

[20]Whether $|\psi_-\rangle$ or $|\psi_+\rangle$ appears in the vibronic ground state depends on the sign of the linear JT coefficient L; $|\psi_-\rangle$ appears if $L > 0$ and $|\psi_+\rangle$ appears if $L < 0$. We regard $|E_\theta\rangle$ and $|E_\epsilon\rangle$ as one-electron kets. Then crystal field theory indicates $L > 0$ and the ground state arises from $|\psi_-\rangle$. If, however $|E_\theta\rangle$ and $|E_\epsilon\rangle$ were defined as single-hole (or many-electron) wave functions, then $L > 0$ and $|\psi_+\rangle$ would have to be taken. Note also that the expectation values of the one-electron Pauli matrices σ_θ and σ_ϵ in the vibronic ground state are those of the operators $-\cos\phi$, $-\sin\varphi$, respectively.

[21]It is instructive to point out that the four long Cu-F bonds of 2.07 Å in $KCuF_3$ reported by Edwards and Peacock (Ref. 9) are the arithmetic mean of the long and short distances given by Okazaki and Suemune (Ref. 7), while the two shorter bonds of 1.96 Å are equal to the intermediate distances given in Ref. 7. Edwards and Peacock (Ref. 9) ascribed their results to a tetragonal distortion of each octahedron in a sense opposite to the commonly found elongated Cu^{2+} and Cr^{2+} complexes.